USE OF WASTE-DERIVED BIOCHAR TO REMOVE COPPER FROM AQUEOUS SOLUTION IN A CONTINUOUS-FLOW SYSTEM

Diego Arán[a,b], Juan Antelo[b,*], Pablo Lodeiro[c], Felipe Macías[a], Sarah Fiol[b,d]

[a]Department of Soil Science and Agricultural Chemistry, University of Santiago de Compostela, 15782 Santiago de Compostela, Spain

[b]Instituto de Investigaciones Tecnológicas, University of Santiago de Compostela, 15782 Santiago de Compostela, Spain

[c]Department of Chemical Oceanography, GEOMAR – Helmholtz Centre for Ocean Research Kiel, 24148 Kiel, Germany

[d]Department of Physical Chemistry, University of Santiago de Compostela, 15782 Santiago de Compostela, Spain

[*]Corresponding author. E-mail: juan.antelo@usc.es

Abstract

The discharges from industrial processes constitute the main source of copper contamination in aqueous ecosystems. In this study we investigated the capacity of different types of biochar (derived from chicken manure, eucalyptus, corncob, olive mill and pine sawdust) to remove copper from aqueous solution in a continuous-flow system. The flow rate of the system strongly influenced the amount of copper retained. [redacted] The physicochemical characteristics of biochar determine the copper retention capacity and the underlying immobilization mechanisms. Biochars with high inorganic contents retain the largest amounts of copper and may be suitable for using in water treatment systems to remove heavy metals. The copper retention capacity of the biochars ranged between ~1.3 and 26 mg g^{-1} and varied in the following order: chicken manure > olive mill >> corncob > eucalyptus > sawdust pine.

Keywords: Sorption, Biochar, Copper, Slow pyrolysis, Continuous-flow systems

1. Introduction

[redacted] Copper is one of the most widely used metals as it is required in many industrial processes (metallurgy, power generation and transmission, electronic manufacturing, mining and agriculture). The waste produced during these processes constitutes the main source of copper and other metals in soils and water.[1] The harmful effects of such contaminants have driven the development of remediation methods based on chemical precipitation, adsorption/co-precipitation on metal oxides, ionic exchange and filtration. [redacted]

The increasing use of inexpensive materials to remove pollutants from the environment has prompted an interest in carrying out adsorption studies aimed at testing different types of material with a view to extrapolating the results to larger scale application. Among the different types of biomass tested for their capacity to scavenge heavy metals, algae and fungi have gained attention because of their elevated retention capacities as well as their wide availability and affordability.[3,4] The use of biochar (BC) as an adsorbent material also represents an inexpensive option for the efficient removal of contaminants from waste water. Biochar is a low-density carbonized material obtained by the combustion of biomass under conditions of low oxygen atmosphere and low temperature.[5] Various types of plant and animal-derived waste have been used to produce BCs in recent years.[6,7] Different studies have demonstrated the ability of BCs to remove Pb, Cu, Zn, Ni and Cr from aqueous solutions.[8-10] Biochar is considered suitable for restoring heavily contaminated environments, such as areas affected by acid mine drainage, because of its high capacity to retain metals.[11] The high retention

capacity is due to the affinity of BC for metal species and to changes in the chemical and physical properties of soil in relation to pH, electric conductivity and cationic exchange capacity. The retention capacity of BC can be due to (i) electrostatic interactions, (ii) ionic exchange, and (iii) sorption by p electrons delocalized from carbon.[12] Most studies that assess the ability of adsorbent materials to retain contaminants are based on batch experiments. However, the performance of these bioadsorbents should also be assessed in continuous systems to provide a more accurate picture of how they act in real situations, e.g. for decontaminating water.[13,14]

Continuous-flow experiments carried out using adsorption columns have provided useful information in addition to that obtained in batch adsorption experiments.[15,16] Ramírez-Pérez et al.[17] performed column experiments to assess the ability of mussel shell amendments to retain heavy metals from a mine soil. These authors concluded that the addition of this waste material to the soil increased the retention capacity and the pH of the soil and decreased the potential desorption of heavy metals. The effects of the physical and chemical properties of the column influent must be established in addition to the optimal operational parameters in order to increase the efficiency of the adsorbent materials. For example, an increase in the ionic concentration and pH of the influent solution led to the removal of more copper from solution when activated carbon was used in fixed-bed columns.[18] Fixed-bed column experiments with an alkali-modified biochar derived from hickory wood showed good immobilization of heavy metals (Pb, Cd, Cu, Zn, Ni) from aqueous solution, and regeneration of the column was possible after washing with acid solution.[19]

The main objective of the present study was to assess the performance of different types of BC to remove copper from an aqueous solution in continuous-flow adsorption columns. For this purpose, BCs were produced by pyrolysis of different types of

feedstock material at low temperature. The specific objectives of the study were (i) to determine the influence of the flow rate on the efficiency of the biochar to remove copper in a continuous flow system, (ii) to determine and compare the capacity of the different types of biochar to retain copper from aqueous solution, and (iii) to determine the relationships between the characteristics of the different types of BC and their copper retention capacity.

2. Materials and Methods

2.1. Preparation and characterization of the biochar samples

Biochars were produced from different types of waste material: chicken manure (CMBC), eucalyptus (EBC), corncob (CCBC), olive mill waste (OBC) and pine sawdust (SBC). The details of the pyrolysis process for CMBC, EBC, CCBC and OBC, as well as the physical treatments applied to the different BCs are described in a previously published paper.[9] Briefly, the BCs were produced by slow pyrolysis at 300ºC for 4 h under oxygen–limited conditions.

Total C, H, N and S contents were determined in an element analyzer (TruSpec CHN-1000, LecoSC-144DR). The ash content was determined by combustion of samples at 1000 ºC for 6 h in muffle furnace (C.H.E. S.A. HT BT S7 RP 1200 ^{0}C). The O content was determined as follows: O (%) = 100 – (C% + H% + N% + S% + Ash%). The surface area (S_{BET}) was determined by N_2 adsorption with a Micromeritics Gemini 2360 V2.01 instrument. The physicochemical characteristics of the different types of BC are summarized in Table 1.

2.2. Fixed–bed column experiments

The continuous flow adsorption experiments were conducted in a glass column, of 15 mm internal diameter and 40 cm length, filled with 5 g of BC. The BC samples were packed in the columns as follows (Figure 1). First, a layer of glass wool was packed in the bottom of the column, to support the fixed bed. A 5 cm layer of acid–cleaned quartz sand (0.5–0.6 mm average particle size) was then placed on top of the glass wool. The central part of the column was packed with the BC samples ([redacted]) to form a layer of thickness 9 cm. Finally, a layer (10 cm thick) of acid-cleaned quartz sand was packed in the top of the column to prevent loss of biomass and to ensure that all of the material was tightly packed. The column was washed with double distilled water for 0.5 h, and a copper solution (5 $mg \cdot L^{-1}$) (prepared from a $Cu(NO_3)_2 \cdot 3H_2O$ salt, Merck) was then fed through the column at different flow rates by a peristaltic pump (Masterflex) connected to the bottom end of the column and operating in up-flow mode. The pH of the copper solution was adjusted to 5.0 ± 0.1 in all experiments by addition of small aliquots of 0.1 M NaOH or HNO_3 solutions.

Several experiments were conducted at different flow rates (2.5, 5.0, 7.0 and 13.0 mL min^{-1}), with CCBC as the sorbent material, to evaluate the effect of the flow rate on the removal of copper from aqueous solution. Subsequent continuous-flow experiments were then carried out at a constant flow rate of 7.0 mL min^{-1}, to compare the capacity of the different types of BC to remove copper from the solution. [redacted]

2.3. Analysis of column data

2.3.1. Mathematical analysis

Copper retention in BC columns was assessed by examination of breakthrough curves, which show the shape of the concentration profile, expressed as the ratio between the concentration of copper in the effluent and in the influent (C/C_0) over time. Numerical integration of the breakthrough curves provides several useful parameters, including the total amount of copper retained by the column, q_{total} (mg), which is expressed by the following equation:

$$q_{total} = \left(\frac{F}{1000}\right)\int_{t=0}^{t=t} C_{ads}\, dt \quad (1)$$

where C_{ads} (mg L^{-1}) is the difference between the initial concentration of copper in the influent (C_0) and the concentration in the effluent (C) at any time; t (min) is the time during which the solution sample circulates through the column, and F (mL min^{-1}) is the flow rate. The amount of copper retained in equilibrium (q_e), expressed in mg g^{-1}, can be calculated as $q_e = q_{total}/M$, where M (g) is the amount of adsorbent material in the column. Other important parameters used to describe the breakthrough curves include the breakthrough point (t_b), which is usually defined as the time needed for the C/C_0 ratio in the effluent to decrease to a value of 0.5 (i.e. so that only 50% of the sorbate remains in the outflowing solution). However, the limiting value of C/C_0 can be established at different values, depending on the purpose and aims of the study and any further applications intended for the effluent. Thus, reductions in the initial concentration of between 3 and 5% have been used by Chen et al. [18] to study copper retention by activated carbon. On the other hand, Lodeiro et al. [3] established an even lower value for this ratio, based on European directives, and recommended specific limits for dissolved Cd in water from industrial effluents. In the present study, the C/C_0 ratio was established as 0.05, which is equivalent to 0.25 mg L^{-1} of copper in the effluent. This value corresponds to the limit for wastewater discharges established by

the [redacted]. [20] This limit is quite strict in view of the range of existing limits in international legislation, which vary from 0.5 to 3 mg L^{-1} for waste water discharges[21, 22], and from 0.05 to 2 mg L^{-1} for water destined for human consumption or for irrigation. [23-25] Additional parameters include the exhaustion time (t_e), defined as the time when the ratio C/C_0 reaches a value of 0.95, and the length of the mass transference front (Z_m), which can be derived from the following equation:

$$Z_m = Z\ (1 - \frac{t_b}{t_e}) \qquad (2)$$

where Z is the length of the column, in cm, and the time interval between t_b and t_e (Δt), known as adsorption zone, is indicative of the rate of mass transfer.

2.3.2. Modelling the breakthrough curves

A non-linear equation based on the Bohart-Adams model[26] was used to fit the breakthrough curves obtained from the column experiments. Despite the premises of its derivation and of its simplicity, the Bohart-Adams model is able to reproduce the experimental breakthrough curves and has been widely used to describe fixed bed continuous-flow systems and to calculate the maximum adsorption capacity of adsorbents. [27,28] Moreover, fitting data to the Bohart-Adams model generally results in lower errors than in other kinetic models such as the Thomas model[29], especially for times far from the breakthrough point. The expression proposed by Yan et al.[26] for the modified Bohart-Adams model, which is based on statistical analysis of experimental data, was used in the present study and is expressed as follows:

$$C/C_0 = 1 - \frac{1}{1 + \left(\frac{C_0 * F}{q_{max} * M} * t\right)^a} \qquad (3)$$

where a is an empirical parameter related to the slope of the regression function and q_{max} is the maximum adsorption capacity of the BC (mg g^{-1}). Both parameters, q_{max} and a, were used as fitting parameters. The models derived from the Bohart-Adams model were only used to describe the experimental breakthrough curves, regardless of theoretical considerations, and to detect any correlations between the model parameters and the experimental variables.

3. Results and Discussion

3.1. Characterization of the biochar samples

The different BC samples were classified according to their C contents, as follows: high C content (85.2%), CCBC; intermediate C content (69.3 and 62.6%), EBC and SBC, and low C content (32.6 and 31.1 %), CMBC and OB. The C content was lowest in the BCs with the highest inorganic contents, i.e. with more than 45% ash (Table 1). The N content varied between 0.41 % and 3.02 %, and the S content between 0.01 % and 0.32 %. The N contents were much higher in the BCs with the lowest C contents, as reported by Ahmad et al.[30], who attributed this finding (which is also applicable to S) to the type of feedstock material used to produce the BC rather than to the pyrolysis conditions.

[redacted] intermediate values

have been reported for different types of BC, e.g. H/C values of 0.67 for BCs derived from peanut shells[33], and values of 0.52 and 0.55 for BC derived from respectively hardwood and corn straw.[34] At the higher end of the range, values of between 1 and 1.4 have been reported for BC derived from pine needles[32] or wood pyrolyzed at low temperature (100-200 ºC).[30] Relative to these previously reported H/C ratios, the values for CCBC are at the lower end of the range, those for SBC are intermediate, and those for EBC, OBC and CMBC are at the upper end of the range.

The O/C molar ratio of the BCs varied between 0.07 and 0.37 (Table 1). High polarity (due to the presence of abundant oxygenated functional groups) leads to high O/C ratios (>0.25), such as those obtained for SBC, CMBC and OBC. On the other hand, O/C ratios ≤0.25, such as those obtained for CCBC and EBC, are indicative of low polarity. O/C values in the range 0.1-0.63 have been reported for BCs elaborated from pine needles, the lowest value corresponding to BC produced by pyrolysis of the material at high temperature (600 ºC) and the highest value for the BC produced by pyrolysis at a lower temperature (100 ºC).[32] Lower O/C values, in the range 0.06-0.107, have been reported for BC derived from wheat residue combusted at different pyrolysis temperatures.[31] The Van Krevelen diagram for the different types of BC in the present study showed that the values of both ratios (H/C and O/C) were within the range of values reported for different types of biochar, derived from plants, animal material or residues such as sewage sludge (Figure S1).

The specific surface area (S_{BET}) data provided a very heterogeneous set of values for the different types of BC (Table 1), ranging from 1.60 $m^2\ g^{-1}$ for EBC to 173 $m^2\ g^{-1}$ for CCBC. The surface area of BC is affected by the nature of the feedstock material and also by pyrolysis conditions, with higher temperatures yielding larger surface areas.

Moreover, pre-treatment with NaOH or KOH facilitates opening and cleaning of the pores, thus also producing a larger surface area.[19,31]

3.2. Effect of flow rate on the optimization of working conditions of the columns

The copper breakthrough curves obtained for the CBCC fixed-bed column at the different flow rates are shown in Fig. 2. An increase in the inflow rate caused a decrease in the saturation time. The parameters derived from the experimental data plotted in the breakthrough curves (Table 2) revealed different relationships with the operational flow rate. Integration of the breakthrough curves for copper adsorption on CCBC led to an increase in q_{total} and Z_m as the flow rate was increased up to 7.0 mL min^{-1}. Nevertheless, no further increase was observed in q_{total} between 7.0 and 13.0 mL min^{-1}, which is consistent with the almost coincident breakthrough curves obtained at both flow rates (Figure 2). Analysis of breakthrough time, t_b, and saturation time, t_e, plotted against the flow rate revealed inverse linear correlations within the interval [redacted] min^{-1} (Figure 3). This finding can be explained by considering that an increase in the flow rate beyond a certain value will reduce the residence time of the solution in the column, thus preventing the solution from reaching the interior of the pores and causing the appearance of the solute in the effluent before the adsorption equilibrium is reached. This effect has been reported for copper and other contaminants at high flow rates.[35,36] The reduction in the flow rate resulted in less steep breakthrough curves (Figure 2) as a consequence of the longer breakthrough and saturation times required for complete exhaustion of the column (Table 2). Parameter Δt was strongly and negatively correlated (R=-0.999) with the flow rate, leading to an increase in the transference zone as the flow rate increases. Taking these results into account, the optimal operational flow rate of the fixed-bed columns was 7.0 mL min^{-1}, and this rate was used in

subsequent experiments carried out to investigate the capacity of the different types of BC to remove copper from aqueous solution.

The modified Bohart-Adams model provided acceptable fits for the experimental data obtained at the different flow rates, with correlations > 0.980 and squared sum of residuals < 0.11 (Figure 2). The fitting parameters are listed in Table 3. The q_{max} value increased linearly with the flow rate ($R^2 > 0.737$). The highest q_{max} value, 5.51 mg g^{-1}, was obtained for a flow rate of 13 mL min^{-1}, and the lowest value, 3.48 mg g^{-1}, corresponded to a flow rate of 2.5 mL min^{-1}. The fitting parameter *a*, which is related to the slope of the regression, varied between 3.2 and 6.7. The decrease in parameter *a* with the increase in flow rate was also linear ($R^2 = 0.978$).

3.3. Comparison of copper sorption on different types of biochar

The copper breakthrough curves obtained with the BC samples under study are shown in Figure 4, and the parameters derived from these curves are shown in Table 4. All experiments were conducted at the same flow rate (7.0 mL min^{-1}) and with a fixed bed height of the adsorbent layer (9 cm). The breakthrough curves show that the BCs can be classified in two groups, with respectively a high and low capacity to remove copper from solution. The BCs with the highest copper retention capacities (CMBC and OBC) corresponded to those with the highest q_e and t_b values, and the BCs with the lowest copper retention capacities (CCBC, EBC, SBC) were those with low q_e and t_b values (Table 4). There was no significant difference in the breakthrough time, t_b, obtained for CMBC and OBC, approximately 45 h. The breakthrough times for the other three samples were all below 10 h. The difference between breakthrough and saturation time, Δt, which is related to the rate of mass transfer, is consistent with the previous classification. The samples with the longest transfer intervals, CMBC and OBC,

produced breakthrough curves with smoother slopes, whereas the slopes for CCBC, EBC and SBC, with shorter transfer intervals, were steeper. Smoother slopes indicate that saturation of the biochar material in the column takes longer. Curves with steeper slopes and short breakthrough times indicate that the retention capacity of the material is relatively low.

Some of the parameters defined by the breakthrough curves were correlated with the physicochemical characteristics of the BCs. In previous batch studies of copper retention on BC, some physicochemical characteristics were found to affect the amount of copper retained.[9] In the present study, copper retention was highest in samples with an O/C molar ratio higher than 0.3 and high ash and phosphorus contents. The mechanism of retention was also found to differ depending on the amount of the inorganic and organic fractions, e.g. the predominance of the mineral fraction over the organic fraction resulted in higher retention capacities due to the combination of adsorption and precipitation processes.

The modified Bohart-Adams model fitted well to the experimental data (Figure 4), yielding R^2 values higher than 0.970 and RRSE lower than 0.10 (Table 5). The q_{max}

values obtained for the different BC materials, i.e. the maximum retention capacity, varied as follow: CMBC > OBC > EBC > CCBC > SBC. The samples with the highest inorganic content, CMBC and OBC, retained more copper: 26.63 and 25.30 mg g^{-1}, respectively. As expected, this parameter was closely correlated with the ash content (R^2 = 0.980). The BC with high organic content, reflected in higher %C and lower ash content, retained less copper, with a decrease in the q_{max} values ranging from 79 to 95 % (Table 5). Parameter *a*, obtained by fitting the modified Bohart-Adams model to the data, was not correlated with the physicochemical properties of the BCs. The values of this parameter ranged between 0.66 for SBC and 9.12 for OBC (Table 5).

The affinity sequence is consistent with the maximum adsorption capacity obtained in batch experiments conducted with the same BCs.[9] A good correlation was observed between the maximum adsorption capacities obtained with the Langmuir-Freundlich model (batch experiments) and those obtained with the modified Bohart-Adams model (continuous experiments) (Figure 5). The maximum retention capacity predicted by the modified Bohart-Adams model was also closely correlated with the breakthrough time (t_b) (R^2=0.991) (Figure S2). The good correlations between parameters enable direct prediction of the behavior of a given biochar in continuous systems and also enable the operational conditions of the columns to be established using the available information obtained in batch experiments.

The copper retention capacity of the BCs were similar to or higher than observed for other BCs. Biochar or activated carbon derived from different types of waste such as pine, pomegranate wood, silver birch, jarrah and wheat straw had similar Cu retention capacities, of between 0.129 mg g^{-1} and 17.83 mg g^{-1}.[18,37-40] CMBC and OBC appear to be the most suitable types of BC for copper retention, because they can remove higher

amounts of Cu from aqueous solution and also because the removal mechanism involves co-precipitation and adsorption, thus producing more stable forms.

4. Conclusions

Flow rate is a key parameter in continuous flow systems with a high adsorption capacity. In the present study, high flow rates (> 7 mL min^{-1}) yielded short breakthrough and saturation times, whereas intermediate to low flow rates provided optimal conditions for retention of copper by BC. Columns filled with CCBC and operating at flow rates of 7 and 5 mL min^{-1} yielded breakthrough times of 5 and 12 hours and maximum copper retention capacities of 3.78 and 4.55 mg g^{-1}, respectively.

The copper retention capacities of the different types of BC tested in the present study were high, with values ranging from 1.28 mg g^{-1} for SBC to 26.63 mg g^{-1} for CMBC. Biochars may therefore be effective and economic alternatives to other sorbent materials for removing heavy metals from aqueous systems. The physicochemical characteristics of the materials used to produce the BCs determine the copper retention capacity and the underlying immobilization mechanisms. The biochars with the highest retention capacity, CMBC and OBC, were also those containing the highest amounts of inorganic compounds. These biochars may be suitable for use in water treatment systems to remove copper or other heavy metals. Finally, a good correlation was observed between the sorption parameters in continuous flow systems and in discontinuous systems. This enables prediction of the behaviour of BC materials and optimization of the operational conditions with very few sorption experiments.

Acknowledgements

The authors belong to the CRETUS Strategic Partnership (AGRUP2015/02), co-funded by FEDER (UE). This work was partially funded by the program Group of Excellence

GI-1245 (GRC2014/003) and by the INTERREG V-A POCTEP Program (0366/RES2VALHUM/1/P). The authors are grateful to Alvaro Gil from the Ceramic Institute of the USC for the BET measurements, David Romero of the Department of Soil Science and Agricultural Chemistry for assistance in the AAS measurements, and the *Centro de Valorización Ambiental del Norte* (Touro, Spain) for preparing the biochar samples.

5. References

(1) Bogusz, A.; Oleszczuk, P.; Dobrowolski, R. Application of Laboratory Prepared and Commercially Available Biochars to Adsorption of Cadmium, Copper and Zinc Ions from Water. *Bioresour. Technol.* **2015**, *196*, 540–549. DOI: 10.1016/j.biortech.2015.08.006

(2) Regmi, P.; García-Moscoso, J.L.; Kumar, S.; Cao, X.; Mao, J.; Schafran, G. Removal of Copper and Cadmium from Aqueous Solution Using Switchgrass Biochar Produced via Hydrothermal Carbonization Process. *J. Environ. Manage.* **2012**, *109*, 61–69. DOI: 10.1016/j.jenvman.2012.04.047

(3) Lodeiro, P.; Herrero, R.; Sastre de Vicente, M. E. Batch Desorption Studies and Multiple Sorption-regeneration Cycles in a Fixed-bed Column for Cd(II) Elimination by Protonated *Sargassum muticum*. *J. Hazard. Mater.* **2006**, *137*, 1649–1655. DOI: 10.1016/j.jhazmat.2006.05.003

(4) Zulfadhly, A.; Mashitah, M. D.; Bhatia, S. Heavy Metals Removal in Fixed-bed Column by the Macro Fungus *Pycnoporus sanguineus*. *Environ. Pollut.* **2001**, *112*, 463–470. DOI: 10.1016/S0269-7491(00)00136-6

(5) Beesley, L.; Marmiroli, M. The Immobilisation and Retention of Soluble Arsenic, Cadmium and Zinc by Biochar. *Environ. Pollut.* **2011**, *159*, 474–480. DOI: 10.1016/j.envpol.2011.07.023

(6) Xu, X.; Cao, X.; Zhao, L. Comparison of Rice Husk- and Dairy Manure-derived Biochars for Simultaneously Removing Heavy Metals from Aqueous Solutions: Role of Mineral Components in Biochars. *Chemosphere* **2013**, *92*, 955–961. DOI: 10.1016/j.chemosphere.2013.03.009

(7) Bird, M. I.; Wurster, C. M.; Silva, P. H. P.; Bass, A. M.; Nys, R. Algal Biochar – Production and Properties. *Bioresour. Technol.* **2011**, *102*, 1886–1891. DOI: 10.1016/j.biortech.2010.07.106

(8) Qiu, Y.; Cheng, H.; Xu, C.; Sheng, G. D. Surface characteristics of crop-residue-derived black carbon and lead (II) adsorption. *Water Res.* **2008**, *42*, 567–574. DOI: 10.1016/j.watres.2007.07.051

(9) Arán, D.; Antelo, J.; Fiol, S.; Macías, F. Influence of Feedstock on the Copper Removal Capacity of Waste-Derived Biochars. *Bioresour. Technol.* **2016**, *212*, 199–206. DOI: 10.1016/j.biortech.2016.04.043

(10) Gupta, V. K.; Ali, I.; Saleh, T. A.; Siddiqui, M. N.; Agarwal, S. Chromium Removal from Water by Activated Carbon Developed from Waste Rubber Tires. *Environ. Sci. Pollut. Res.* **2013**, *20*, 1261–1268. DOI: 10.1007/s11356-012-0950-9

(11) Garrido-Rodriguez, B.; Cutillas-Barreiro, L.; Fernández-Calviño, D.; Arias-Estévez, M.; Fernández-Sanjurjo, M.J.; Álvarez-Rodríguez, E.; Núñez-Delgado, A. Competitive Adsorption and Transport of Cd, Cu, Ni and Zn in a Mine Soil Amended with Mussel Shell. *Chemosphere* **2014**, *107*, 379–385. DOI: 10.1016/j.chemosphere.2013.12.097

(12) Sohi, S.P.; Krull, E.; Lopez-Capel, E.; Bol, R. A Review of Biochar and its Use and Function in Soil. *Adv. Agron.* **2010**, *105*, 47–82. DOI: 10.1016/S0065-2113(10)05002-9

(13) Callery, O.; Healy, M.G.; Rognard, F.; Barthelemy, L.; Brennan, R. B. Evaluating the Long-Term Performance of Low-Cost Adsorbents Using Small-Scale Adsorption

Column Experiments. *Water Res.* **2016**, *101*, 429–440. DOI: 10.1016/j.watres.2016.05.093

(14) Sadaf, S.; Bhatti, H. N. Batch and Fixed Bed Column Studies for the Removal of Indosol Yellow BG Dye by Peanut Husk. *J. Taiwan Inst. Chem. Eng.* **2014**, *45*, 541–553. DOI: 10.1016/j.jtice.2013.05.004

(15) Patrón-Prado, M.; Lodeiro, P.; Lluch-Cota, D. B.; Serviere-Zaragoza, E.; Casas-Valdez, M.; Zenteno-Savín, T.; Méndez-Rodríguez, L. Efficiency of Copper Removal by *Sargassum sinicola* in Batch and Continuous Systems. *J Appl. Phycol.* **2013**, *25*, 1933–1937. DOI: 10.1007/s10811-013-0031-6

(16) Park, J. H.; Cho, J. S.; Ok, Y. S.; Kim, S. H.; Kim, S. H.; Kang, S. W.; Choi, I. W.; Heo, J. S.; DeLaune, R. D.; Seo, D. C. Competitive Adsorption and Selectivity Sequence of Heavy Metals by Chicken Bone-Derived Biochar: Batch and Column Experiment. *J. Environ. Sci. Health, Part A: Toxic/Hazard. Subst. Environ. Eng.* **2015**, *50*, 1194–1204. DOI: 10.1080/10934529. 2015.1047680

(17) Ramírez-Pérez, A. M.; Paradelo, M.; Nóvoa-Muñoz, J. C.; Arias-Estévez, M.; Fernández-Sanjurjo, M. J.; Álvarez-Rodríguez, E.; Núñez-Delgado, A. Heavy Metal Retention in Copper Mine Soil Treated with Mussel Shells: Batch and Column Experiments. *J. Hazard. Mater.* **2013**, *248-249*, 122–130. DOI: 10.1016/j.jhazmat.2012.12.045

(18) Chen, J. P.; Yoon, J. T.; Yiacoumi, S. Effects of Chemical and Physical Properties of Influent on Copper Sorption onto Activated Carbon Fixed-Bed Columns. *Carbon* **2003**, *41*, 1635–1644. DOI: 10.1016/S0008-6223(03)00117-9

(19) Ding, Z.; Hu, X.; Wan, Y.; Wang, S.; Gao, B. Removal of Lead, Copper, Cadmium, Zinc, and Nickel from Aqueous Solutions by Alkali-Modified Biochar: Batch and Column Tests. *J. Ind. Eng. Chem*. **2016**, *33*, 239–245. DOI: 10.1016/j.jiec.2015.10.007

(20) Business for Social Responsibility, *BSR Water Quality Guidelines*. http://www.bsr.org/reports/awqwg/BSR_AWQWG_Guidelines-Testing-Standards.pdf. (accessed May 15, 2017).

(21) EC, Directive 2010/75/EC of the European Parliament and of the Council - on Industrial Emissions. *Official Journal European Communities* **2010**, *334*, 17–119.

(22) BIS IS 2490-1, Tolerance Limits For Industrial Effluents Discharged Into Inland Surface Waters - Part 1: General Limits. *Bureau of Indian Standard*. **1981**.

(23) WHO, Copper in drinking water. Background Document for Development of WHO Guidelines for Drinking-water Quality (WHO/SDE/WSH/03.04/38). *World Health Organization*, Genève. **2004**.

(24) EC, Directive 98/83/EC of the Council - on the Quality of Water Intended for Human Consumption. *Official Journal of the European Communities* **1998**, *330*, 32–54.

(25) US-EPA, Maximum Contaminant Level Goals and National Primary Drinking Water Regulations for Lead and Copper; Final Rule. *US Environmental Protection Agency. Federal Register*, **1991**, *56*, 26460–26564.

(26) Yan, G.; Viraraghavan, T.; Chen, M. A New Model for Heavy Metal Removal in a Biosorption Column. *Adsorpt. Sci. Technol.* **2001**, *19*, 25–43. DOI: 10.1260/0263617011493953

(27) Chu, K. H. Fixed Bed Sorption: Setting the Record Straight on the Bohart-Adams and Thomas Models. *J. Hazard. Mater.* **2010**, *177*, 1006–1012. DOI: 10.1016/j.jhazmat.2010.01.019

(28) Kiran, B.; Kaushik, A. Cyanobacterial Biosorption of Cr(VI): Application of Two Parameter and Bohart Adams Models for Batch and Column Studies. *Chem. Eng. J.* **2008**, *144*, 391–399. DOI: 10.1016/j.cej.2008.02.003

(29) Han, R.; Wang, Y.; Zhao, X.; Wang, Y.; Xie, F.; Cheng, J.; Tang, M. Adsorption of Methylene Blue by Phoenix Tree Leaf Powder in a Fixed-Bed Column: Experiments and Prediction of Breakthrough Curves. *Desalination* **2009**, *245*, 284–297. DOI: 10.1016/j.desal.2008.07.013

(30) Ahmad, M.; Rajapaksha, A. U.; Lim, J. E.; Zhang, M.; Bolan, N.; Mohan, D.; Vithanage, M.; Lee, S. S.; Ok, Y. S. Biochar as a Sorbent for Contaminant Management in Soil and Water: A Review. *Chemosphere* **2014**, *99*, 19–33. DOI: 10.1016/j.chemosphere.2013.10.071

(31) Chun, Y.; Sheng, G.; Chiou, C. T.; Xing, B. Compositions and Sorptive Properties of Crop Residue-Derived Chars. *Environ. Sci. Technol.* **2004**, *38*, 4649–4655. DOI: 10.1021/es035034w

(32) Chen, B.; Zhou, D.; Zhu, L. Transitional Adsorption and Partition of Nonpolar and Polar Aromatic Contaminants by Biochars of Pine Needles with Different Pyrolytic Temperatures. *Environ. Sci. Technol.* **2008**, *42*, 5137–5143. DOI: 10.1021/es8002684

(33) Ahmad, M.; Lee, S. S.; Dou, X.; Mohan, D.; Sung, J.; Yang, J. E.; Ok, Y. S. Effects of Pyrolysis Temperature on Soybean Stover- and Peanut Shell- Derived Biochar Properties and TCE Adsorption in Water. *Bioresour. Technol.* **2012**, *118*, 536–544.

DOI: 10.1016/j.biortech.2012.05.042

(34) Chen, X.; Chen, G.; Chen, L.; Chen, Y.; Lehmann. J.; McBride, M. B.; Hay, A. G. Adsorption of Copper and Zinc by Biochars Produced from Pyrolysis of Hardwood and Corn Straw in Aqueous Solution. *Bioresour. Technol*. **2011**, *102*, 8877–8884. DOI: 10.1016/j.biortech.2011.06.078

(35) Sağ, Y.; Nourbakhsh, M.; Aksu, Z.; Kutsal, T. Comparison of Ca-alginate and Immobilized *Z. ramigera* as Sorbents for Copper (II) Removal. *Process Biochem*. **1995**, *30*, 175–181. DOI: 10.1016/0032-9592(95)80009-3

(36) Ahmad, A. A.; Hameed, B. H. Fixed-bed Adsorption of Reactive Azo Dye onto Granular Activated Carbon Prepared from Waste. *J. Hazard. Mater.* **2010**, *175*, 298–303. DOI: 10.1016/j.jhazmat.2009.10.003

(37) Komkiene, J.; Baltrenaite, E. Biochar as Adsorbent for Removal of Heavy Metal Ions [Cadmium(II), Copper(II), Lead(II), Zinc(II)] from Aqueous Phase. *Int. J. Environ. Sci. Technol.* **2016**, *13*, 471–482. DOI: 10.1007/s13762-015-0873-3

(38) Muhamad, H.; Doan, H.; Lohi, A. Batch and Continuous Fixed-bed Column Biosorption of Cd^{2+} and Cu^{2+}. *Chem. Eng. J.* **2010**, *158*, 369–377. DOI:10.1016/j.cej.2009.12.042

(39) Ghaedi, A. M.; Ghaedi, M.; Vafaei, A.; Iravani, N.; Keshavarz, M.; Rada, M.; Tyagi, I.; Agarwal, S.; Gupta, V. K. Adsorption of Copper (II) Using Modified Activated Carbon Prepared from Pomegranate Wood: Optimization by Bee Algorithm and Response Surface Methodology. *J. Mol. Liq.* **2015**, *206*, 195–206. DOI: 10.1016/j.molliq.2015.02.029

(40) Alslaibi, T. M.; Abustan, I.; Azmier, M.; Foul, A. A. Kinetics and Equilibrium Adsorption of Iron (II), Lead (II), and Copper (II) onto Activated Carbon Prepared from Olive Stone Waste. *Desalin. Water Treat.* **2014**, *52*, 7887–7897. DOI: 10.1080/19443994.2013.833875

Figure captions

Figure 1. Experimental set-up of adsorption columns

Figure 2. Breakthrough curves for Cu removal by CCBC at different flow rates. Symbols represent the experimental data points and lines represent the modified Bohart-Adams model fit

Figure 3. Variation in breakthrough, t_b, and exhaustion, t_e, times in relation to the flow rate

Figure 4. Breakthrough curves for Cu removal by different types of BC at a constant flow rate 7 mL min^{-1}. Symbols represent the experimental data points and lines represent the modified Bohart-Adams model

Figure 5. Correlation between the maximum retention capacities predicted by the empirical models for batch and continuous flow experiments. Q_{max} values obtained with the Lagmuir-Freundlich model are taken from Arán et al. (2016)

Table captions

Table 1. Physico-chemical characteristics of the different types of biochar

Table 2. Parameters obtained from the breakthrough curves of copper adsorption by CCBC at different flow rates

Table 3. Parameters obtained from the non-linear fit of the modified Bohart-Adams model to the breakthrough curve for CCBC

Table 4. Parameters obtained from the breakthrough curves of copper adsorption by different types of BC at a constant flow rate of 7.0 mL min^{-1}

Table 5. Parameters obtained by fitting the modified Bohart-Adams model to the breakthrough curves for the different BCs

Table 1. Physico-chemical characteristics of the different types of biochar.

	CMBC	OBC	EBC	CCBC	SBC
%C	32.6	31.1	69.3	85.2	62.6
%N	3.02	2.10	0.41	0.80	0.67
%H	3.90	2.40	5.10	2.10	3.67
%S	0.32	0.08	0.01	0.10	0.04
%Ash	46.4	49.5	1.90	3.90	2.13
%O	13.7	14.8	23.2	7.90	30.8
O/C	0.32	0.35	0.25	0.07	0.37
H/C	1.45	0.94	0.88	0.29	0.70
S_{BET} (m^2 g^{-1})	1.79	3.80	1.60	173.0	43.28

Table 2. Parameters obtained from the breakthrough curves of copper adsorption by CCBC at different flow rates.

Flow (mL min^{-1})	**13.0**	**7.0**	**5.0**	**2.5**
q_t (mg)	32.16	32.14	24.46	18.22
q_e (mg g^{-1})	6.43	6.64	4.89	3.64
t_b (h)	3.08	5.17	11.66	18.25
t_e (h)	19.54	24.0	31.00	39.63
Z_m (cm)	7.58	7.06	5.61	4.83
Δt (h)	15.96	18.83	20.00	21.38

Table 3. Parameters obtained from the non-linear fit of the modified Bohart-Adams model to the breakthrough curve for CCBC.

Flow rate (mL min^{-1})	q_{max} (mg g^{-1})	a	R^2	RRS
13	5.51 ± 0.06	3.2 ± 0.1	0.995	0.023
7.0	3.78 ± 0.03	4.6 ± 0.2	0.992	0.036
5.0	4.55 ± 0.06	5.6 ± 0.3	0.988	0.045
2.5	3.48 ± 0.04	6.7 ± 0.4	0.984	0.102

Table 4. Parameters obtained from the breakthrough curves of copper adsorption by different types of BC at a constant flow rate of 7.0 mL min^{-1}.

Type of BC	CCBC	CMBC	OBC	EBC	SBC
q_{total} (mg)	32.14	136.98	124.35	26.79	14.87
q_e (mg g^{-1})	6.64	27.40	24.87	5.36	2.97
t_b (h)	5.17	47.00	47.25	9.50	0.25
t_e (h)	24.0	86.00	82.00	25.30	16.00
Z_m (cm)	7.06	4.08	3.81	5.62	8.86
Δt (h)	18.83	39.00	34.75	15.80	17.75

Table 5. Parameters obtained by fitting the modified Bohart-Adams model to the breakthrough curves for the different BCs.

	q_{max} (mg g^{-1})	a	R^2	RRSE
CMBC	26.6 ± 0.26	6.43 ± 0.46	0.978	0.042
OBC	25.3 ± 0.11	9.12 ± 0.36	0.992	0.022
EBC	5.28 ± 0.08	6.40 ± 0.52	0.978	0.008
CCBC	3.78 ± 0.03	4.62 ± 0.19	0.992	0.036
SBC	1.28 ± 0.07	0.66 ± 0.03	0.980	0.007

Graphical Abstract

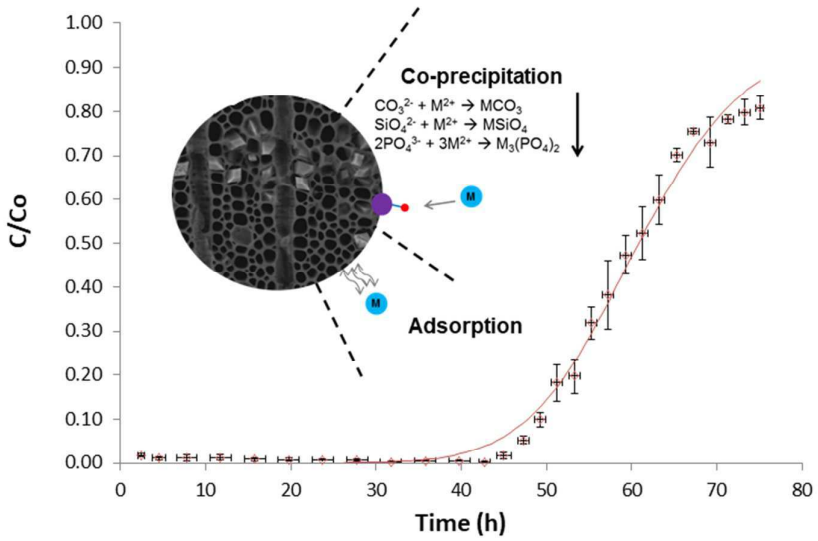

Figure 1. Experimental set-up of adsorption columns

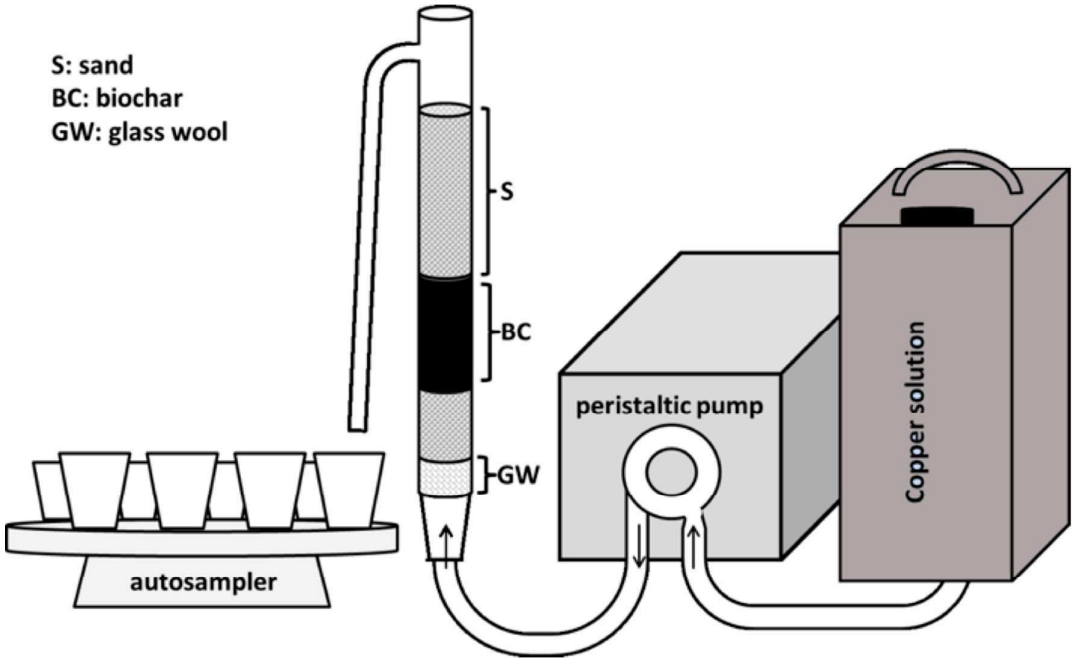

Figure 2. Breakthrough curves for Cu removal by CCBC at different flow rates. Symbols represent the experimental data points and lines represent the modified Bohart-Adams model fit

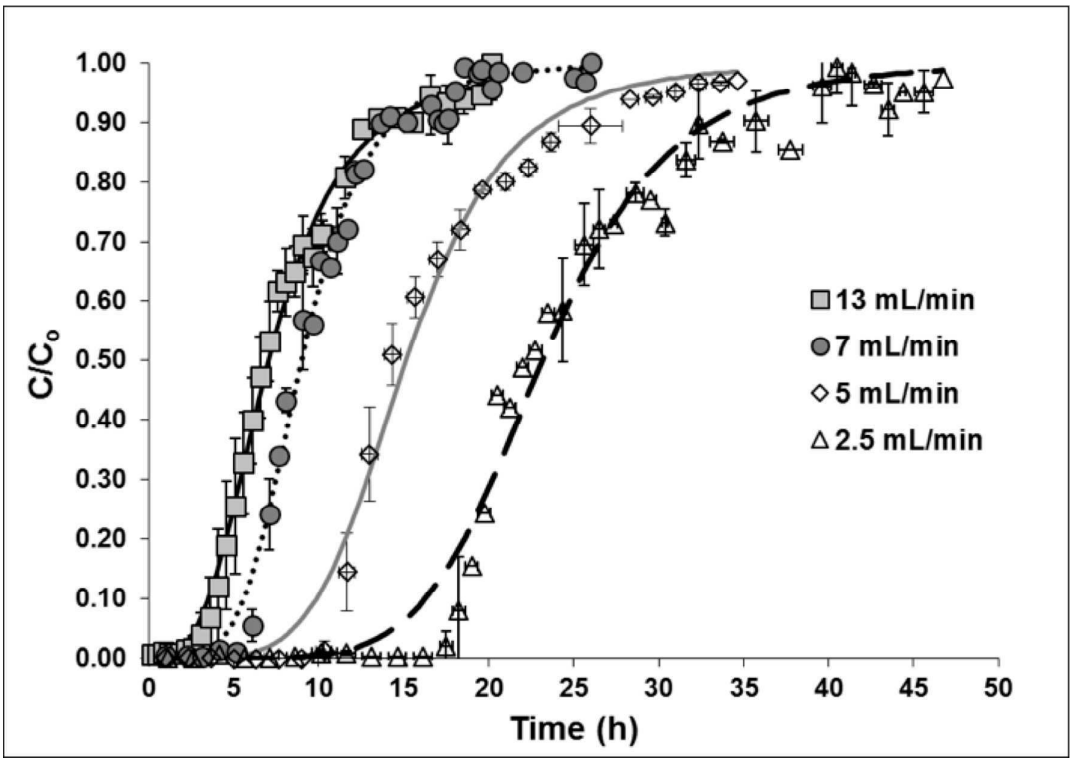

Figure 3. Variation in breakthrough, t_b, and exhaustion, t_e, times in relation to the flow rate

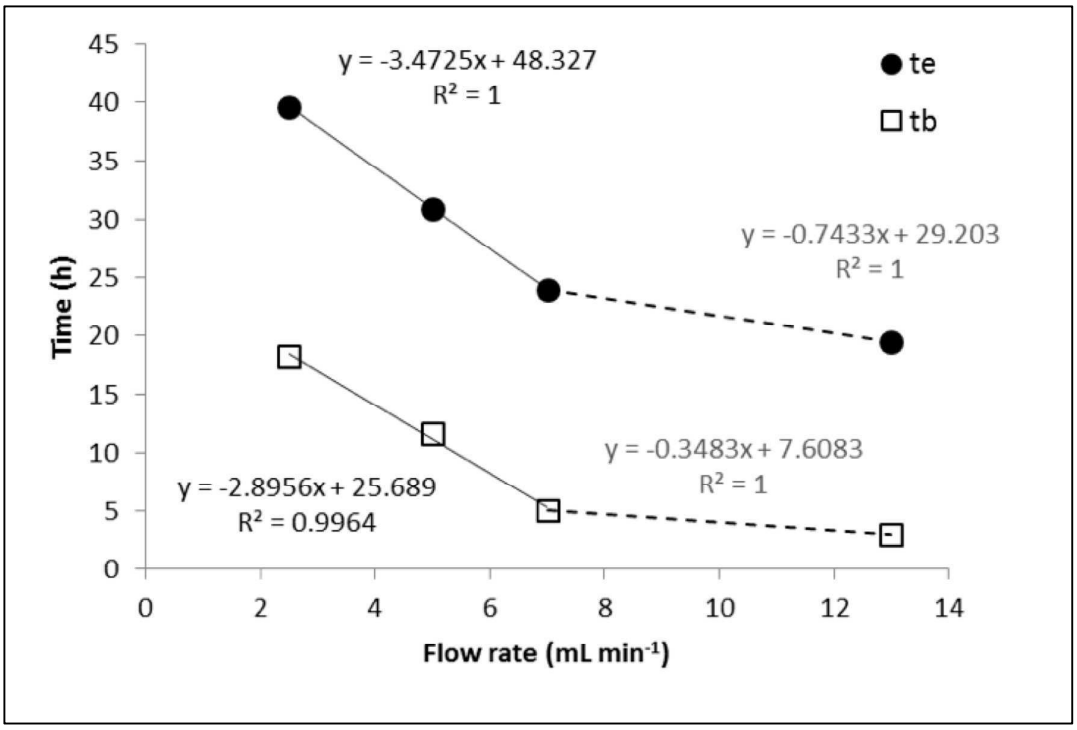

Figure 4. Breakthrough curves for Cu removal by different types of BC at a constant flow rate 7 mL min^{-1}. Symbols represent the experimental data points and lines represent the modified Bohart-Adams model

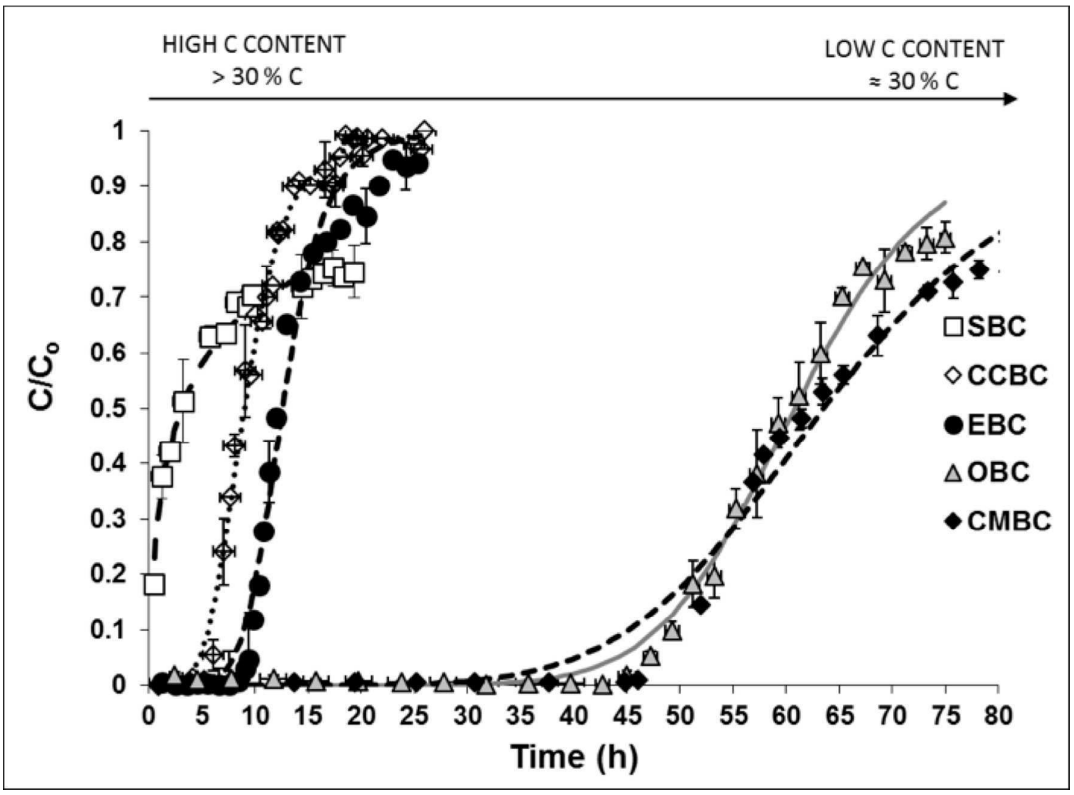

Figure 5. Correlation between the maximum retention capacities predicted by the empirical models for batch and continuous flow experiments. Q_{max} values obtained with the Lagmuir-Freundlich model are taken from Arán et al. (2016)